Available online at www.sciencedirect.com
ScienceDirect
Wear 263 (2007) 1585–1592
WEAR
www.elsevier.com/locate/wear

# The effect of oil pockets size and distribution on wear in lubricated sliding

Waldemar Koszela, Pawel Pawlus *, Lidia Galda

*Rzeszow University of Technology, Poland*

Received 14 August 2006; received in revised form 29 December 2006; accepted 1 January 2007
Available online 23 May 2007

**Abstract**

The paper reviews the current efforts being made on surface texturing and presents a literature analysis about running-in process of sliding components.

The wear resistance test is described. The results of experimental investigations of the oil pockets (created by burnishing technique) existence effects on tribological performance of sliding elements under mixed lubrication conditions are presented. The block made from bronze contacted the steel ring. The wear intensity, friction coefficient and roughness were measured during the tests. Surface texturing of the block surface (area density between 20 and 26%) resulted in significant improvement in wear resistance in comparison to a system with a turned block.

The paper deals also with the commonly observed behavior involving running-in followed by steady wear. We compared total wear rate of sliding elements and coefficient of friction in initial wear period with those during steady-state. It was found that running-in affected steady wear. When textured surface topography was removed, the equilibrium roughness was reached independently of the initial roughness.


*Keywords:* Oil pockets; Running-in; Steady wear; Friction; Wear rate

## 1. Introduction

Surface texturing emerged as an option of surface engineering resulting in improvement in load capacity, coefficient of friction, wear resistance, etc. Various techniques can be employed for surface texturing including machining, ion beam texturing, etching techniques and laser texturing [1]. The oil pockets (also known as micropits, holes, dimples or cavities) may reduce friction in two ways: by providing lift themselves as a micro-hydrodynamic bearing, and also by acting as a reservoir of lubricant [2]. Holes can also serve as a micro-trap for wear debris in lubricated or dry sliding [1].

The most familiar practical examples include plateau honed cylinder surfaces in combustion engines. The two-process surface is created. The authors of article [3] obtained the proportionality between cylinder oil capacity and engine oil consumption. Santochi and Vignale [4] stated that increase of oil capacity improved engine performance. Jeng [5] found that friction coefficient under mixed lubrication condition of two-process surface was smaller than that of one process surface, when $R_q$ parameters of two analysed surfaces were the same. Now laser surface texturing is successfully applies to cylinder liners [6,7]. Surface texturing was observed to reduce the coefficient of friction [6], oil consumption and cylinder wear during running-in [7] compared to non-textured liners.

The benefits of applying laser surface texturing to piston rings were demonstrated theoretically and experimentally [8,9]. The results of theoretical work showed a potential reduction of friction force of about 30% by ring surface texturing in comparison to non-textured rings under full lubrication conditions [8]. These results were confirmed experimentally [9].

Surface texturing is also successfully applied to mechanical seals resulting in increase in seal life [10]. It was found that partial laser surface texturing improved substantially load-carrying capacity of hydrodynamic thrust bearings [11]. Surface texturing is also used extensively in metal forming [2].

A majority of researchers found that surface texturing of contacting elements reduced the frictional force substantially

* Corresponding author. Tel.: +48 17 8631536; fax: +48 17 8651184.
*E-mail address:* ppawlus@prz.rzeszow.pl (P. Pawlus).

0043-1648/$ – see front matter © 2007 Elsevier B.V. All rights reserved.
doi:10.1016/j.wear.2007.01.108

in comparison to untextured surfaces. Surface texturing was observed to expand the range of hydrodynamic lubrication regime [12–14].

Surface texturing resulted in minimizing the surface ability to seizure [15,16]. The dimples existence from area density of 10% improved seizure resistance of sliding pair: steel–spheroidal cast iron [16].

Textured surfaces can provide traps for wear debris in dry contacts subjected to fretting. The dimple existence could improve the fretting wear resistance [17] and almost doubled the fretting fatigue life [18].

We found little information about the effect of dimple existence on improvement of tribological properties of journal bearings, although textured bearing sleeves are produces by some firms (for example, Glacier) and are recommended to work under mixed lubrication conditions. Only a few papers were concerned with the effect of oil pockets on wear intensity.

The dimples of mainly spherical shape are usually formed on stationary surface of smaller hardness. Three dimensions characterise surface texturing: diameter, depth and area density. Extensive literature survey revealed that usually dimple depth over dimple diameter ratio range of 0.01–0.3 and area density to 30% exist for assemblies operated in lubricated sliding conditions. The laser texturing is the most popular technique in forming micropits. However other methods may be used. Impulse burnishing can be a very promising approach. In this technique special endings act as hammers to form oil pockets on metal surfaces.

Accommodation of sliding surfaces over a period of time (running-in, breaking-in, shakedown, wearing-in) causes changes of their initial surface topography. The term running-in is used more in Europe, while term breaking-in tends to be favored in the United States. The running-in process enables machines to improve surface topography and frictional compatibility. Running-in characteristics for a machine assembly are affected by its design, fitting-up during assembly, and its history of prior use.

Several criteria can be employed to characterise the running-in completion. These include stable roughness, steady wear and steady friction. The time needed to reach a steady rate of wear and that to achieve a steady-state of friction may not necessarily be equal [19].

During running-in the wear removal or plastic deformation (initial stage of running-in) can take place [20].

Past research revealed that obtaining longer life for engines relied on a suitable running-in process [21]. Surface roughness is the main factor that influence the running-in if there are no apparent surface defects.

Kragelsky et al. defined the end of running-in in terms of the number of cycles to reach the optimum load-carrying capacity of a surface, and that involved surface roughness [22].

During the ‘zero-wear’ process the wear volume or wear loss is within the limits of the original surface topography of the component and is hard to determine [23]. Initial surface topography affects running-in period, running-in wear intensity and sometimes steady wear.

The wear intensity is often proportional to initial surface height. Usually the bigger surface topography height causes bigger wear during running-in, after this period the wear intensity is constant [24]. The wear of cylinder surfaces during running-in was proportional to the initial roughness height [25].

It was found that initial cylinder surface topography affected its wear not only during running-in, but also when the wear amount was big [26]. The consequence of the removal of oil pockets from surface of cylinders is dangerous for the engine, because leads to engine failure.

Usually surface topography height decreased during running-in [19,22–25,27]. Qualitative three-dimensional characterisation of cylinder surface wear was done by Dong and Stout [27]. They were marked changes in skewness and kurtosis. However some authors found increase of roughness height during initial period of wear. The authors of paper [28] observed the increase in roughness height during collaboration of metals of different hardness, even during lubrication.

It is believed that surface roughness obtained after running-in does not depend on initial surface height. When solid contact occurs, smooth surfaces tend to get rougher and rougher surfaces tend to get smoother (equilibrium surface roughness [22]). Some authors reported an optimum initial surface roughness (after machining). Becker and Ludema [29] obtained similar values of the $R_a$ parameter of various cylinders tested on Cameron-Plint tribometer (duration of the test was 1 h). The authors of paper [30] found that the wear rate increased with increasing roughness though the final roughness of all specimens reached the same roughness. Whatever surface roughness begins on a surface, roughness changes to a roughness that is characteristic of the system and its running conditions. So the machined surface should be similar to worn surface (after finishing “zero-wear”).

However different results were also mentioned. For example the authors of paper [31] analysed the change in surface roughness during running-in of partial elastohydrodynamic lubricated wear. Specimen surfaces with different roughness ended up with different roughness after running-in. The larger the initial roughness, the larger the final roughness.

## 2. The aims and scope of the investigations

The fundamental aim of the investigations is to study the effect of dimple size and distribution on wear in lubricated sliding.

The second aim is to analyse the influence of initial wear period on tribological performance of sliding components.

The co-action between bearing sleeve and journal was simulated using block-on ring tester. Dimples were created on the stationary block surface by impulse burnishing (embossing) technique.

## 3. Experimental procedure

### 3.1. The test apparatus

The experiments were conducted on a block-on ring tester as shown in schematic representation of Fig. 1. The tribosystem

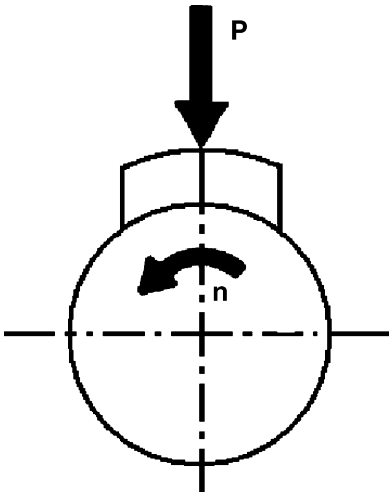


Fig. 1. The scheme of the tested assembly.

consists of the stationary block (specimen) pressed at the required load $P$ against the ring (counter-specimen) rotating at the defined speed. The temperature of the test block can be measured using thermocouple. The construction allows us to measure the friction force between ring and block. This tester can simulate some real practical machinery, particularly slide bearings. We tried to simulate co-action between bearing sleeve and journal, therefore this tester was used.

Fig. 2 shows the laboratory stand.

### 3.2. Specimens

The specimens were made from bronze B101 (CuSn10P) of 138 HB hardness and chemical constitution shown in Table 1. The material was selected because it is commonly used for bearing sleeves.

The inner specimen surface (collaborated with counter-specimen) was obtained after precise turning to $Ø35^{+0.05}$ diameter.

Machined specimen surfaces were modified using burnishing techniques in order to obtain surfaces with circular oil pockets

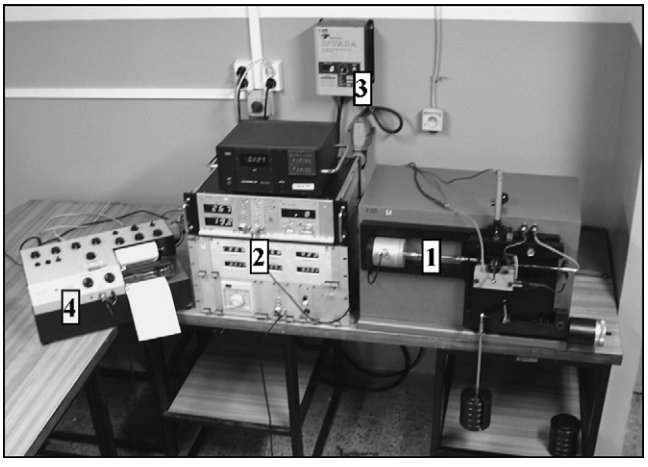


Fig. 2. The photo of the laboratory stand: 1, tribological tester; 2, system of measurement and control; 3, speed governor; 4, recorder of measurement results.

Table 1
Chemical constitution of bronze B101

| | |
|---|---|
| Alloying constituents (%) | |
| Sn | 9–11 |
| P | 0.5–1 |
| Cu | Rest |
| Allowable impurities (max, %) | |
| Pb | 1.2 |
| Sb | 0.3 |
| Fe | 0.3 |
| Zn | 0.6 |
| S | 0.05 |

(see Fig. 3). The dimple size and distribution were selected initially in order to obtain the area density (ratio) in the range of 10–90%. Usually smaller dimple area ratio is used. But we would like also to analyse the effect of surface layer hardening (not only surface topography) on wear.

The oil pockets depth to diameter ratios were between 0.03 and 0.11. This range was recommended in the literature. Specimen surface had dimples with depths ranging from 45 to 115 μm. Dimples depths were comparatively big since oil pockets should exist on the surfaces during test; the wear conditions were very severe (assumed wear amounts of specimens were about 100 μm).

### 3.3. Counter-specimens

Counter-specimens were made from 40HM steel, of hardness 40 HRC obtained after heat treatment. Chemical constitution of rings is given in Table 2. This material is frequently used for journals. After heat treatment (in order to obtain necessary hardness), grinding was done. During grinding the outer surface (collaborated with specimen surface), the specially prepared device with conic base surface was used for precise counter-specimens preparation.

### 3.4. Lubricant

The experiments were conducted under lubricated sliding conditions. The lubricant was machine oil L-AN 46 (mineral oil, refined by anti-foaming, anti-oxidizing and anti-corrosive agents).

Table 3 gives the physical properties of used lubricant.

Table 2
Chemical constitution of steel 40HM

| | |
|---|---|
| Alloying constituents (%) | |
| C | 0.38–0.45 |
| Mn | 0.4–0.70 |
| Si | 0.17–0.37 |
| Cr | 0.90–1.20 |
| Mo | 0.15–0.25 |
| Allowable impurities (max, %) | |
| P | 0.035 |
| S | 0.035 |
| Ni | 0.33 |

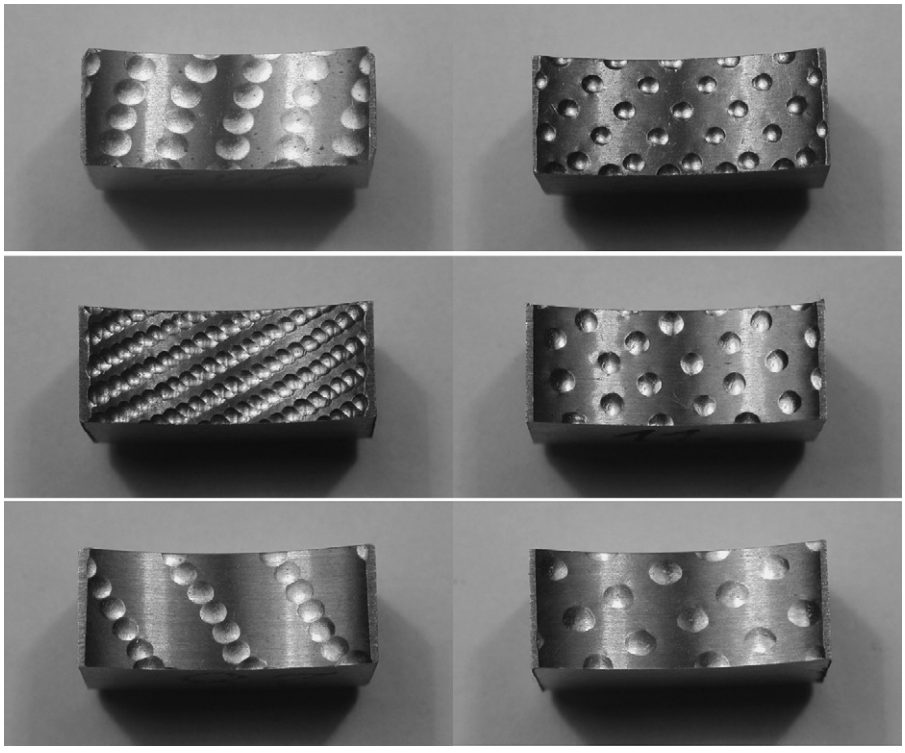

Fig. 3. Examples of specimen surfaces before tribologic test.

The selected oil is commonly used for different machine elements, therefore it was selected for tribological tests.

### 3.5. Test procedure

During the test, the total linear wear (displacement) of the assembly: specimen–counter-specimen was measured. The friction force was continuously measured with the force transducer. The temperature of the test block surface was measured with a thermocouple. Before and after the tests the topography of the sliding surfaces was measured by stylus profilometry Surtronic 3+ (in axial direction—across the lay), the counter-specimen diameter was measured and the sliding surfaces were investigated using optical microscopy Epityp 2. Having measurement before and after test provides only limited information about the process. Therefore wear rate $I_{hL}$ was also calculated. It describes the dynamics of changes of characteristic dimensions during wear. $I_{hL}$ was obtained according to following formula:

$$I_{hL} = \frac{\Delta Z}{L} \text{mm/km}$$

Table 3
The parameters of L-AN 46 oil

| Parameters | Values |
|---|---|
| Viscosity index | min 60 |
| Ignition temperature (°C) | min 170 |
| Kinematic viscosity in 40 °C ($mm^2/s$) | 41.4–50.6 |
| Flow temperature (°C) | −27 |
| Density in 40 °C ($kg/m^3$) | 880 |

where $I_{hL}$ is the linear wear rate; $\Delta Z$ the change of linear dimensions of the tested assembly between measuring points; $L$ is the sliding distance between measuring points.

The conditions of tests were more severe than in the majority of similar assemblies in real situations. Selection of test conditions was determined by assumed test duration.

The described test procedure was the result of initial experiments. It took the minimisation of errors (inaccuracy of specimen and counter-specimen execution, errors caused by linear expansion of contacting elements) into consideration. The discontinuous test simulated process of starting and stoppage of the real sliding assembly: bearing sleeve—journal under mixed lubrication conditions. The normal load was 1500 N (unitary pressure 15 MPa), sliding velocity was 0.22 m/s, total sliding distance was about 5 km. After specified sliding distances the spindle was stopped and joint linear wear of the tested assembly was measured.

The obtained results were compared with results of specimens without oil pockets (after precise turning).

## 4. Results and discussion

The results of total wear values of specimens and counter-specimens, maximum friction force after run duration (specified sliding distances), and roughness parameters before and after wear were studied. Hardness as well as the results of the microscopic observations of sliding surfaces were also analysed.

Wear values of counter-specimens were small (up to 3 μm). The results of total wear rates of analysed assemblies are

Table 4
The results of measurement of final wear values and wear rates of tested specimens (mean values)

| Assembly number | Final wear (μm) | Wear rate vs. sliding distance (mm/km) | | | | | |
|---|---|---|---|---|---|---|---|
| | | $0.22 \times 10^3$ m | $0.66 \times 10^3$ m | $1.76 \times 10^3$ m | $2.86 \times 10^3$ m | $3.96 \times 10^3$ m | $5.06 \times 10^3$ m |
| Series 0 (not modified) | 121 | 0.173 | 0.032 | 0.010 | 0.017 | 0.019 | 0.016 |
| Series 1 | 107 | 0.059 | 0.025 | 0.025 | 0.020 | 0.016 | 0.014 |
| Series 2 | 156 | 0.114 | 0.043 | 0.035 | 0.025 | 0.025 | 0.015 |
| Series 3 | 92 | 0.059 | 0.027 | 0.018 | 0.016 | 0.013 | 0.014 |
| Series 4 | 136 | 0.086 | 0.043 | 0.035 | 0.011 | 0.030 | 0.014 |
| Series 5 | 190 | 0.209 | 0.054 | 0.037 | 0.035 | 0.015 | 0.021 |
| Series 6 | 137 | 0.095 | 0.034 | 0.020 | 0.022 | 0.022 | 0.027 |
| Series 7 | 123 | 0.086 | 0.023 | 0.015 | 0.021 | 0.027 | 0.022 |
| Series 8 | 148 | 0.123 | 0.052 | 0.024 | 0.020 | 0.024 | 0.021 |

displayed in Table 4. The experiment (for each series) was repeated three times and mean values are presented.

The measured wear of assembly with not modified (after precise turning) specimen were the reference data (series 0). The analysis of wear of tested assembly revealed intensive wear in first stage and its stabilisation in second stage. The wear rates in successive stages were rather similar. So we reached steady-state wear after running-in—see Fig. 4. The coefficient of friction of sliding pair with not-modified specimen amounted to 0.1–0.123. The roughness of specimen surface characterised by $R_a$ parameter after finishing wear resistance test was about 0.35 μm.

We will present the result of all series tests for three groups of assemblies. Group 1 contains sliding pairs (series 4, 6, 7) for which wear after sliding distance of $5.06 \times 10^{-6}$ m was similar to assembly of series 0 (with not modified specimen). Specimens from series 4 were characterised by average individual dimple diameter of 1050 μm, depth of 115 μm and area density of 88.3%, from series 6 by average diameter of 1550 μm, depth of 45 μm and area density of 36.8%, but from series 7 by average diameter of 1050 μm, a depth of 115 μm and area density of 9.8%. The wear rates during running-in were in the range 0.086–0.095 mm/km, but during steady-state wear between 0.011 and 0.022 mm/km. The results are shown in Fig. 5. The coefficients of friction amounted respectively to

- 0.117–0.143—for series 4.
- 0.12–0.137—for series 6.
- 0.11–0.133—for series 7.

Because wear amounts were bigger than initial oil pockets depths, the resulted surfaces after tests did not contain dimples. Final surface roughness $R_a$ parameters were in the range 0.52–0.58 μm.

The second group includes assemblies characterised by bigger wear values (variants 2, 5, 8). Block samples no. 2 had oil pockets with average diameter of 1050 μm, depth of 115 μm (sizes of individual dimples) and area density of 40.7%, no. 5—average diameter of 1050 μm, depth of 115 μm and area density of 66.6%, but no. 8—average diameter of 1550 μm, depth of 45 μm and area density of 75.2%.

The total wear values were in the range 148–190 μm. The wear intensity during running-in was bigger than that of assemblies from the first group, in the range 0.114–0.209 mm/km. But steady wear value was similar to that of group 1: 0.015–0.025 mm/km (see Fig. 6). The friction coefficients were bigger than in the first group and amounted to:

- 0.137–0.153—for series 2.

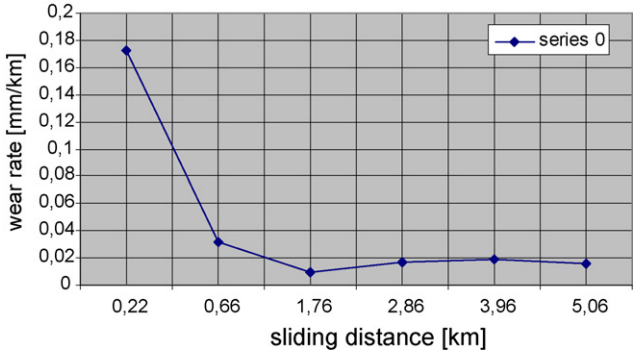


Fig. 4. The graph of mean wear rates vs. sliding distance of assembly from series 0.

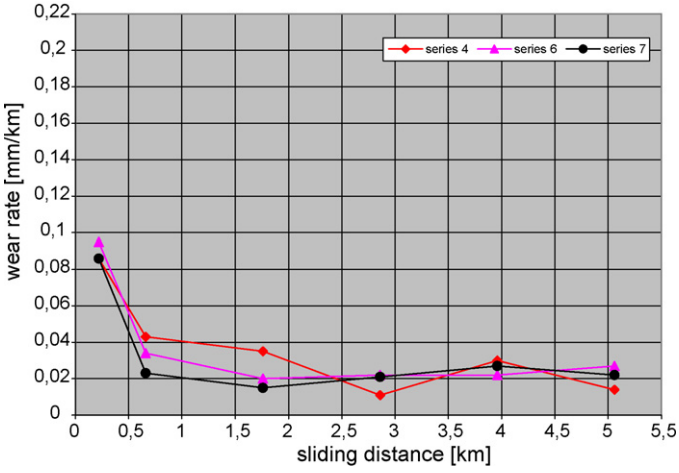


Fig. 5. The graph of mean wear rates vs. sliding distance of assemblies from series 4, 6, 7.

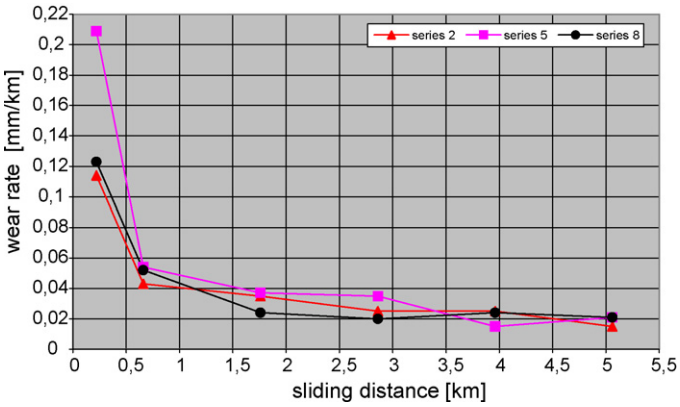


Fig. 6. The graph of mean wear rates vs. sliding distance of assemblies from series 2, 5, 8.

- 0.127–0.147—for series 5.
- 0.1–0.127—for series 8.

Final surface roughness $R_a$ parameters were similar to those from previously analysed group and amounted to: 0.5–0.6 μm. The oil pockets were not visible on surfaces after finishing wear resistance test.

Group 3 contains assemblies (series 1—dimples diameter 1550 μm, depth 45 μm, area density 19.2% and 3—dimples diameter 1050 μm, depth 115 μm, area density 20.4%), for which the linear wear was the smallest from all the analysed series. The wear values of these sliding pairs were respectively 107 and 92 μm.

The wear intensity during running-in was 0.059 mm/km (smaller than of other groups), but during steady wear it was similar to other analysed groups and amounted to 0.014–0.025 mm/km. The results are presented in Fig. 7. The coefficients of friction were smaller than in presented above cases and amounted to:

- 0.1–0.127—for series 1
- 0.097–0.11—for series 3.

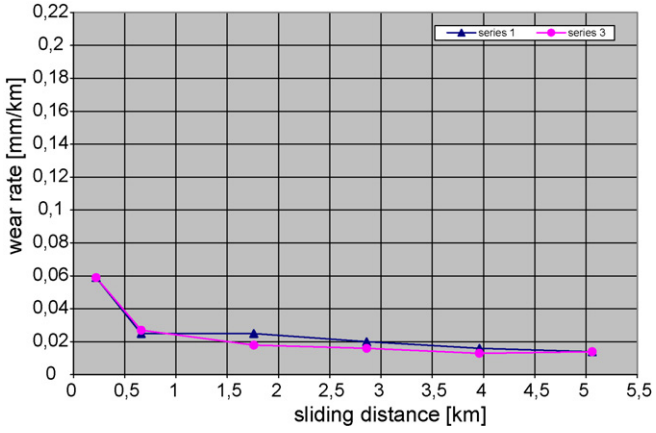


Fig. 7. The graph of mean wear rates vs. sliding distance of assemblies from series 1 and 3.

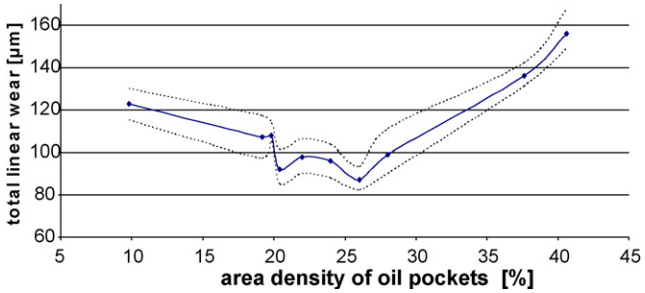


Fig. 8. The effect of oil pockets area density on total linear wear of the analysed assembly (95% confidence interval).

Specimen surfaces from series 1 did not contain the holes after finishing tests, their roughness height $R_a$ was on average 0.42 μm. We observed the oil pockets on worn surfaces from block no. 3, roughness height $R_a$ parameter was equal 0.84 μm, although we tried to exclude dimples from the roughness measurement.

Burnishing surface texturing with area density of 20.4% was observed to reduce total linear wear of the tested assembly of 24% when compared to untextured surfaces. Therefore the additional experiment was done. Dimples area ratios were in the range: 19.9–27.8%. When oil pockets existed on worn surfaces, the final values of $R_a$ parameter were in the range 0.8–0.92 μm, in the other cases 0.52–0.64 μm. The smallest wear (88 μm) was obtained for dimple area density of 25.9%, average diameter of 1050 μm and depth of 115 μm. So surface texturing minimised linear wear of the tested assembly by 27% in comparison to a system with a turned block.

Generally we obtained the smallest wear values (88, 92 μm) for the deepest dimples (115 μm). Fig. 8 presents the effect of area density (range 9.8–40.7%) of oil pockets on specimen surface on total linear wear of the tested sliding pair. The increase in wear during increase in dimples area ratio more than 30% was caused by increase of unitary pressure. So oil pockets area ratio should not be very big, because it could cause increase of unitary pressures, intensification of adhesive joints and increase of wear intensity. The further decrease of wear for oil pockets area range 75.2–88.3% is the probable result of surface layer hardening. But the effect of initial surface topography seems to be more important than the effect of physical properties of the outer layer. The further details are given in Ref. [32].

After the analysis of presented above Figs. 4–7 it was found that the total wear value depended on the wear during running-in. The sliding pairs of bigger (smaller) total linear wear (running-in and steady-state wear) were also characterised by bigger (smaller) wear rates during running-in. So running-in is important with regard to minimisation of steady-state wear. Of course the obtained results depend on the ratio of running-in and steady wear duration.

Fig. 9 presents the dependence between total linear wear of the assembly: specimen–counter-specimen and maximum value of the coefficient of friction in the final wear stage.

The coefficient of friction is proportional to wear (the coefficient of determination is 0.73). Maximum values of friction forces between sliding surfaces are presented in Table 5. The

Table 5
The results of maximum friction forces (mean values)

| Assembly number | Maximum friction force vs. sliding distance ($N$) | | | | | |
|---|---|---|---|---|---|---|
| | $0.22 \times 10^3$ m | $0.66 \times 10^3$ m | $1.76 \times 10^3$ m | $2.86 \times 10^3$ m | $3.96 \times 10^3$ m | $5.06 \times 10^3$ m |
| Series 0 (not modified) | 165 | 145 | 150 | 175 | 185 | 180 |
| Series 1 | 190 | 170 | 165 | 160 | 155 | 150 |
| Series 2 | 205 | 225 | 230 | 210 | 205 | 215 |
| Series 3 | 165 | 155 | 150 | 145 | 150 | 145 |
| Series 4 | 175 | 180 | 185 | 200 | 215 | 210 |
| Series 5 | 190 | 195 | 215 | 210 | 220 | 215 |
| Series 6 | 190 | 180 | 180 | 190 | 200 | 205 |
| Series 7 | 165 | 180 | 195 | 200 | 185 | 185 |
| Series 8 | 150 | 150 | 155 | 165 | 180 | 190 |

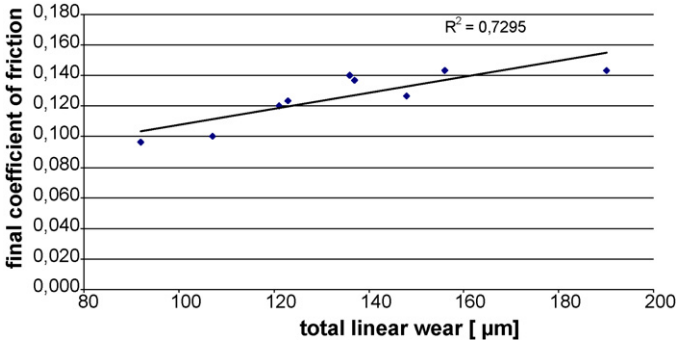


Fig. 9. Dependence between total linear wear of the analysed assembly and maximum coefficient of friction in the end of the test.

maximum friction force of assemblies from group 3 (series 1 and 3) declined during the test and reached a stable value. The time needed to obtain a steady wear rate and steady-state of friction was similar. However the maximum friction force between other sliding pairs increased versus sliding distance. Stabilisation of friction force was found after stabilisation of wear. In general, the maximum friction coefficient curves are similar to block temperature curves.

The microscopic observations revealed that the oil pockets were filled in by wear debris. The roughness heights $R_a$ of the worn specimens without oil pockets were in the range: 0.42–0.6 μm (average value 0.46 μm). The roughness amplitudes of worn counter-specimens from the same sliding pairs were similar ($R_a$ was in the range 0.4–0.6 μm; before wear test $R_a$ was 0.39 μm). A significant reduction in the surface roughness height of specimens was obvious from the measurement (the initial oil pockets depths were between 45 and 115 μm). However roughness amplitude of worn specimen surfaces was similar to roughness height of not-modified surface before the test ($R_a$ was initially 0.54 μm). Spacing parameter $R_{Sm}$ increased from 28 μm (surface after precise turning) to the range 73–132 μm. This is the consequence of creating one-directional worn structure. Roughness height of worn specimens from having dimples was bigger—$R_a = 0.8$–$0.92$ μm (of counter-specimens 0.6–0.9 μm). The specimen roughness increase can be the consequence of getting out wear debris from oil pockets. When oil pockets were removed the smoothing mechanism of surfaces occurred, but the roughness heights of worn textured specimen were still bigger than those of worn surface of turned specimens (series 0): $R_a = 0.34$ μm (the $R_a$ parameter of worn counter-specimen surface in this case was comparatively small—0.28 μm). Maybe the stabilisation of the roughness and its decrease to values characteristic to worn not initially textured surfaces of the co-acting parts would take place if the test duration was bigger. So probably the time needed to obtain stable roughness (characteristic of the system and its operating conditions) is bigger than the time to obtain steady-states of wear and friction.

However generally the roughness height of initially textured surfaces after finishing "zero-wear" did not depend on the initial (burnished) roughness amplitude.

## 5. Conclusions

Surface texturing of the block surface (area density between 20 and 26%) by burnishing technique resulted in significant improvement in wear resistance in comparison to a system with untextured samples. The area ratio of 26% minimised linear wear of the tested assembly by 27% in comparison to a system with a turned block. However the oil pockets area ratio should not be very big, because it could cause increase of unitary pressures and then increase of wear intensity. The smallest wear was obtained for the biggest dimple depth.

The running-in process affects running-in duration, and wear during running-in, but can also influence the steady wear value. The results obtained during wear-resistance test of sliding elements confirmed the last sentence. Wear rates of various analysed assemblies during running-in were different, but during steady wear similar. The steady-state wear was found to be significantly influenced by running-in wear rate. Control of the running-in process can be a substantial tool in extending the life of engineering components. The coefficient of friction is correlated with linear wear and wear intensity. Stabilisation of friction (in most cases) and then of roughness were found after stabilization of wear. When textured surface topography was removed, the equilibrium roughness was reached independently of the initial roughness.

## References

[1] I. Etsion, State of the art in laser surface texturing, ASME J. Tribol. 125 (2005) 248–253.

[2] B. Nilsson, B.-G. Rosen, T.R. Thomas, D. Wiklund, L. Xiao, Oil pockets and surface topography: mechanism of friction reduction, in: Proceedings of the XI International Colloquium on Surfaces, Chemnitz, Germany, 2004 (Addendum).
[3] S.P. Hill, T.C. Kantola, J.R. Browa, J.C. Hamelink, An experimental study of the effect of cylinder bore finish on engine oil consumption. SAE Paper 950938, 1568–1576.
[4] M. Santochi, M. Vignale:, A study on the functional properties of a honed surface, CIRP Ann. 31 (1982) 431–434.
[5] Y. Jeng, Impact of plateaued surfaces on tribological performance, Tribol. Trans. 39/2 (1996) 354–361.
[6] G. Duffet, P. Sallamand, A.B. Vannes, Improvement in friction by cw Nd:YAG laser surface treatment on cast iron cylinder bore, Appl. Surf. Sci. 205 (2003) 289–296.
[7] S. Brinkman, H. Bodschwinna, Characterisation of automotive bore performance using 3D surface metrology, in: L. Blunt, X. Jiang (Eds.), Advanced Techniques for Assessment Surface Topography, Kogan Page Science, London and Sterling, 2003, pp. 307–347.
[8] A. Ronen, I. Etsion, Y. Kligernman, Friction-reducing surface texturing in reciprocating automotive components, Tribol. Trans. 44/3 (2001) 359–366.
[9] G. Ryk, Y. Kligernman, I. Etsion, Experimental investigation of laser surface texturing for reciprocating automotive components, Tribol. Trans. 45/4 (2002) 444–449.
[10] Surface Technologies Ltd. URL http://surface-tech.com.
[11] V. Brizmer, Y. Kligerman, I. Etsion:, A laser surface textured parallel thrust bearing, Tribol. Trans. 46/3 (2003) 397–403.
[12] X. Wang, K. Kato, K. Adachi, K. Aizawa, The effect of laser texturing of SiC surface on the critical load for the transition from water lubrication mode from hydrodynamic to mixed, Tribol. Int. 34 (2001) 703–711.
[13] X. Wang, K. Kato, K. Adach, K. Lizawa, Load carrying capacity map for the surface design of SiC thrust bearing sliding in water, Tribol. Int. 36 (2003) 189–197.
[14] A. Kovalchenko, O. Ajayi, A. Erdemir, G. Fenske, I. Etsion, The effect of laser surface texturing on transitions in lubrication regimes during unidirectional sliding contact, Tribol. Int. 38 (2005) 219–225.
[15] X. Wang, K. Kato, Improving the anti-seizure ability of SiC seal in water with RIE texturing, Tribol. Lett. 14/4 (2003) 275–280.
[16] L. Galda, W. Koszela, D. Stadnicka, P. Pawlus, The improvement of machine elements functional properties by oil pockets creation on collaborating surfaces, in: Proceedings of the AUSTRIB 2006 Conference, Brisbane, Australia, 2006, p. 46.
[17] M. Varenberg, G. Halperim, I. Etsion, Different aspects of the role of wear debris in fretting wear, Wear 252 (2002) 902–910.
[18] A. Volchok, G. Halperin, I. Etsion, The effect of surface regular topography on fretting fatigue life, Wear 253 (2002) 509–515.
[19] P.J. Blau, On the nature of running-in, Tribol. Int. 38 (2005) 1007–1012.
[20] K.L. Johnson, Contact mechanics and the wear of metals, Wear 190 (1995) 162–170.
[21] M. Priest, C.M. Taylor, Automobile engine tribology—approaching the surface, Wear 241 (2000) 193–203.
[22] I.V. Kragelsky, M.N. Dobychnin, V.S. Kombalov:, Friction and Wear Calculation Methods, Pergamon Press, 1982.
[23] K. Kaliszer, G.W. Rowe, G. Trmal, On the relationship between wear and surface topography, CIRP Ann. 22/2 (1973) 284–290.
[24] G. Masouros, A. Dimarogonas, K. Lefas, A model for wear and surface roughness transients during the running-in of bearings, Wear 45 (1977) 375–383.
[25] P. Pawlus, A study on the functional properties of honed cylinder surface during running-in, Wear 176 (1994) 247–254.
[26] P. Pawlus, Effects of honed cylinder surface topography on the wear of piston–piston ring–cylinder assemblies under artificially increased dustiness conditions, Tribol. Int. 26 (1) (1994) 49–56.
[27] W.P. Dong, K.J. Stout, An integrated approach to the characterization of surface wear. I. Qualitative characterization, Wear 181–183 (1995) 700–716.
[28] J. Sugimura, Y. Kimura, K. Amino, Analysis of the topography changes due to wear—geometry of the running-in process, JSLE 31/11 (1986) 813–820.
[29] E.P. Becker, K.C. Ludema, A qualitative empirical model of cylinder bore wear, Wear 225–229 (1999) 387–404.
[30] R. Kumar, B. Prakash, A. Sethuramiah, A systematic methodology to characterise the running-in and steady-state wear process, Wear 252 (2002) 445–545.
[31] W. Wang, P.L. Wong, Z. Zhang, Experimental study of the real time change in surface roughness during running-in for PEHL contact, Wear 244 (2000) 140–146.
[32] W. Koszela, Impulse burnishing of cylindrical surfaces in friction condition, Ph.D. Dissertation, Rzeszow University of Technology, Rzeszow, Poland, 2003 (in Polish).